

W-Band Complex Permittivity Measurements at High Temperature Using Free-Space Methods

Martin S. Hilario, Brad W. Hoff[✉], Member, IEEE, Benmaan Jawdat, Michael T. Lanagan[✉], Zane W. Cohick, Frederick W. Dynys, Jonathan A. Mackey, and Joseph M. Gaone

Abstract—Free-space measurement techniques can be contactless and are able to accommodate large, flat sheets of dielectric material, making them useful for characterization of high-temperature, millimeter-wave, window and radome candidate materials. As part of the present work, a high-temperature, W-band (75–110 GHz), free-space measurement system was developed and used to characterize complex dielectric properties of bulk material samples at temperatures ranging from 25 °C to 600 °C. Two test cases, polyvinyl chloride (PVC) and CoorsTek 92% alumina, were measured at 25 °C and found to have ϵ'_r values of 2.731 ± 0.005 and 8.061 ± 0.027 at 95 GHz, respectively. The 25 °C PVC sample was measured to have a ϵ''_r value of 0.032 ± 0.007 . At 25 °C, the ϵ''_r value of the 92% alumina sample was below the uncertainty threshold achievable with the present free-space measurement apparatus and could only be bounded to <0.009 . As the alumina sample was heated to 600 °C, ϵ'_r and ϵ''_r values increased to 8.501 ± 0.028 and 0.035 ± 0.008 , respectively. The high-temperature behavior of the authors' 92% alumina ceramic was found to be similar to that previously documented for Sumitomo AKP-50 alumina over the 25 °C–600 °C temperature range. In addition to the 92% alumina sample, three commercially available ceramic substrates (zirconium oxide, boron nitride, and silicon nitride) were also characterized at temperatures ranging from 25 °C to 600 °C.

Index Terms—Ceramics, complex permittivity, dielectric losses, dielectric measurement, dielectric substrates, high temperature, polymers.

I. INTRODUCTION

TO SUPPORT the development of W-band (75–110 GHz) source technology, radomes, absorbers, and other W-band dielectric components, such as those described in [1]–[3], millimeter (mm)-wave dielectric-property data are required for dielectric insulators at both 25 °C and at elevated

Manuscript received February 24, 2018; revised March 20, 2019; accepted April 12, 2019. Date of publication April 23, 2019; date of current version June 6, 2019. This work was supported by the Air Force Office of Scientific Research under Grant FA9550-17RDCOR449. Recommended for publication by Associate Editor M. Cases upon evaluation of reviewers' comments. (*Corresponding author: Brad W. Hoff*)

M. S. Hilario, B. W. Hoff, and B. Jawdat are with the Air Force Research Laboratory, Kirtland Air Force Base (AFB), Albuquerque, NM 87117 USA (e-mail: brad.hoff@us.af.mil).

M. T. Lanagan and Z. W. Cohick are with the Department of Materials Science and Engineering, Pennsylvania State University, University Park, PA 16802 USA.

F. W. Dynys and J. A. Mackey are with the NASA Glenn Research Center, Cleveland, OH 44135 USA.

J. M. Gaone is with the Worcester Polytechnic Institute, Worcester, MA 01609 USA.

Color versions of one or more of the figures in this paper are available online at <http://ieeexplore.ieee.org>.

Digital Object Identifier 10.1109/TCMT.2019.2912837

temperatures. A variety of techniques to characterize complex dielectric properties at microwave and mm-wave frequencies have been described in the literature [4]–[8]. These techniques include the use of resonant cavity spectroscopy [9]–[25], dielectric-filled waveguide transmission [26]–[30], interferometry [13], [14], [26], [31]–[52], open waveguide (coaxial or other) probes [13], [26], [53], [54], and free-space methods [7], [26], [55]–[77].

W-band dielectric property data at 25 °C for many materials, including solid polymers [5], [6], [11]–[13], [16], [18]–[21], [26], [28], [31], [35]–[37], [40], [50], [54], [55], [58], [59], [61]–[63], [65], [66], [68], [72]–[76], [78], non-magnetic ceramics [5], [6], [9], [11], [16], [26], [31], [33], [35]–[38], [48]–[52], [55], [59], [60], [65], [71], [77], [79], ferrite ceramics [41]–[45], semiconductors [34], [49], [80], food grains [46], and liquids [6], [17], [20], [21], [25], [47], [48], [60], [81], [82], are relatively abundant in the literature; however, sources of mid-temperature (up to 200 °C) [9], [18] and high-temperature (>200 °C) [11], [12], [19], [83] dielectric-property data at frequencies within or approaching W-band are relatively scarce. Calame *et al.* [9], Garven *et al.* [18], Ho [21], Westphal and Sils [11], and Westphal [12] utilize resonant cavity techniques to obtain their high-temperature dielectric-property data.

As noted by Venkatesh and Raghavan [4], the sample preparation for resonant-cavity spectroscopy tends to be more difficult compared to other measurement techniques and can require destruction of larger test pieces since high-frequency measurements require small sample sizes with a specific geometry. In contrast, free-space techniques are contactless; can accommodate large, flat sheets of sample material; and, thus, allow for comparatively easy sample preparation. For measurements of low-loss materials, however, the free-space method will tend to incur larger uncertainties than techniques like resonant cavity spectroscopy [4], [7].

Measurement of high-temperature, complex dielectric-property data (both ϵ'_r and ϵ''_r) using free-space techniques has been reported previously for Ka-band (26.5–40 GHz) [70] and Ku-band (12–18 GHz) frequencies [69]. Lemaire *et al.* [64] describe the development of an X-band and W-band free-space system capable of measuring permittivity at elevated temperatures; however, values for imaginary permittivity (ϵ''_r) could not be extracted at W-band. Because of the comparative benefits of utilizing free-space measurement techniques, the Air Force Research Laboratory developed a W-band, high-

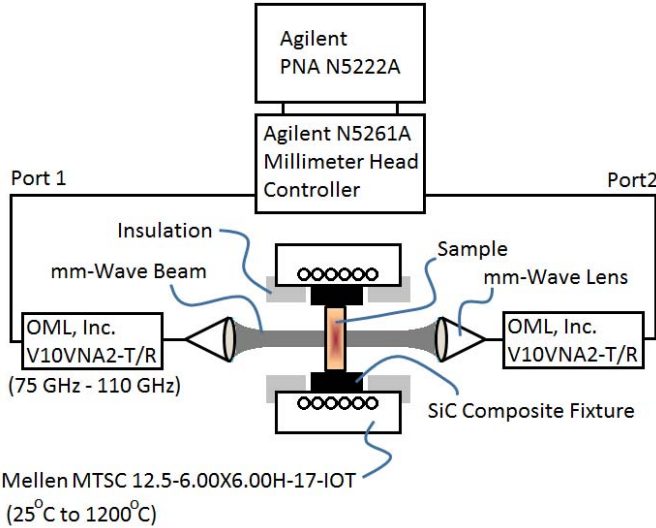


Fig. 1. Schematic depiction of the high-temperature experimental apparatus.

temperature, free-space measurement apparatus capable of measuring complex permittivity. This apparatus is, effectively, an evolution of Varadan's configuration [69], which utilizes modern components and is adapted for higher frequencies.

II. APPARATUS

A schematic representation of the experimental apparatus used for the mm-wave measurements is depicted in Fig. 1. The Agilent performance network analyzer (PNA) 5222A network analyzer forms the core of the measurement system. An Agilent N5261A millimeter head controller and a set of OML V10VNA-T/R frequency extender heads (one for each port) serve to boost the output of the PNA base unit to W-band frequencies (75–110 GHz). The WR-10 waveguide output from each of the frequency extender heads feeds a matched set of custom-designed, lensed, spot-focusing horn antennas.

When high-temperature measurements are to be performed, the sample is located in the center of a Mellen tube furnace, which has an overall length and diameter of 31.75 and 15.24 cm, respectively, and was designed with a 15.24-cm-long, uniform heating region centered along the axial length of the furnace. The furnace is capable of a maximum temperature of 1200 °C; however, for the reported experiments, a maximum temperature of 600 °C is utilized. Silicon carbide composite sample holders with apertures large enough to accommodate 5.08-, 7.62-, and 10.16-cm-diameter samples were used for experimentation. A photograph of the experimental setup is provided in Fig. 2.

Temperature measurements are made with a thermocouple embedded in the sample holder immediately adjacent to the outer radius of the sample. Temperature uncertainty comprises the inherent uncertainty of the thermocouple measurements (± 2.5 °C) combined with the maximum temperature differential between the edge of the sample and the center of the sample, observed at 600 °C for all samples measured in the present study ($\Delta = 5$ °C), as measured with a thermal imaging

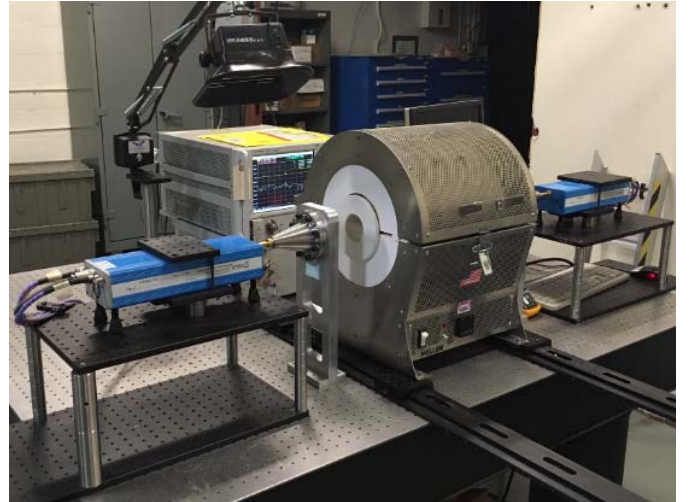


Fig. 2. Photograph of the high-temperature experimental apparatus.



Fig. 3. Photograph of millimeter-wave, spot-focusing antennas, each with a WR-10 connector and interface compatible with either a vacuum chamber or open air.

camera. In the present configuration, the thermal imaging camera cannot be used to view the sample when mm-wave measurements are being performed.

A. Spot-Focusing Lens Design

The matched pair of Gaussian, spot-focusing antennas used for the present experiments are shown in Fig. 3. The antennas were designed by Millitech, Inc. with a center frequency of 94 GHz, but allow for broadband operation in the W-band frequency range (75–110 GHz). Each antenna is composed of a WR-10 input terminal connected to a corrugated horn and quartz lens. The lens face is vacuum sealed to an 11.43-cm Conflat flange [81]. The beam waist diameter was specified to be 3.40 cm at the focal point, which is located 33.0 cm from the front of the lens. The sample is centered at the focal point, where the wavefront approximates a plane wave. A plot of the measured beam waist diameter as a function of distance from the lens flange is provided in Fig. 4.

Separation of the lenses from the furnace assembly allows for the use of forced-air cooling to maintain the lenses at near-room temperature. This cooling method is effective up to furnace temperatures of 600 °C. Beyond that temperature,

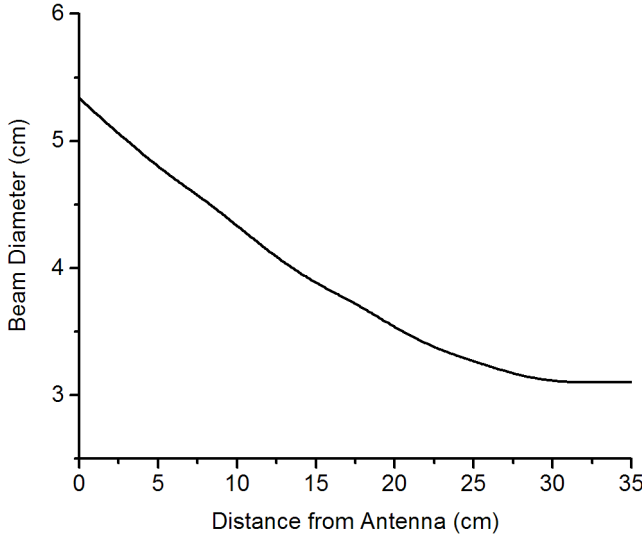


Fig. 4. Beam waist ($1/e^2$) diameter measurements of 94-GHz millimeter-wave horn antennae.

infrared output from the furnace interior begins to overwhelm the present forced-air cooling method used for the lenses.

III. PARAMETER EXTRACTION

The vector network analyzer was calibrated in a two-step process using the through-reflect-line (TRL) [84] standard at the waveguide ports and a gated-reflect-line (GRL) [85] compensation routine to remove the error contributions of the antennas from the propagation and reflection parameters. A flat aluminum plate was used as a calibration standard for the gating procedure.

Dielectric properties of the sample materials can be described in terms of the real and imaginary components of the complex dielectric constant, ϵ_r^* , which is related to complex permittivity ϵ^* , given by

$$\epsilon^* = \epsilon_0 \epsilon_r^* = \epsilon_0 (\epsilon_r' - i \epsilon_r'') \quad (1)$$

where ϵ_0 is the free-space permittivity, ϵ_r' is the real part of the complex dielectric, and ϵ_r'' is the imaginary part of the dielectric constant. The real and imaginary parts of the relative permittivity are related to the loss tangent by

$$\tan \delta = \frac{\epsilon_r''}{\epsilon_r'}. \quad (2)$$

The S-parameters for each test material were measured in a GRL-calibrated free-space electromagnetic beam setup and numerically converted to the real and imaginary parts of permittivity. These S-parameters are related to the transmission and reflection coefficients. Assuming symmetry between opposite ports (S_{11} and S_{22} , S_{21} and S_{12}), the relationships are given by the following equations:

$$S_{11} = \frac{\Gamma(1 - T^2)}{1 - \Gamma^2 T^2} \quad (3)$$

$$S_{21} = \frac{T(1 - \Gamma^2)}{1 - \Gamma^2 T^2} \quad (4)$$

where the transmission (T) and reflection (Γ) coefficients of a planar propagating wave through a sample material of thickness d are

$$T = e^{-\gamma d} \quad (5)$$

$$\Gamma = \frac{z - 1}{z + 1}. \quad (6)$$

The transmission and reflection coefficients are related to the complex relative permittivity ϵ_r^* and complex relative permeability μ_r^* by the propagation constant (γ) and characteristic impedance (z) given by

$$\gamma = \gamma_0 \sqrt{\mu_r^* \epsilon_r^*} \quad (7)$$

$$\gamma_0 = \frac{2\pi i}{\lambda_0} \quad (8)$$

$$z = \sqrt{\frac{\mu_r^*}{\epsilon_r^*}} \quad (9)$$

where γ_0 is the free-space propagation constant and λ_0 is the wavelength in free space.

The power transmission and reflection coefficients are given by the squares of the transmission and reflection coefficient, respectively, and the absorbed power is given by

$$P_{\text{abs}} = 1 - |T|^2 - |\Gamma|^2. \quad (10)$$

The S-parameters for each test material are measured in a GRL-calibrated free-space electromagnetic beam setup and numerically converted to the real and imaginary parts of permittivity. Complex permittivity and permeability can be calculated from S_{11} and S_{21} parameters using least-squares fitting to the transmission-line equations, as in [86].

IV. EXPERIMENTAL RESULTS

Two experimental testing series were performed. First, dielectric-property measurements of a 0.64-cm-thick CoorsTek 92% α -Alumina (α -Al₂O₃) sample and a polyvinyl chloride (PVC) sample were performed at 25 °C using a sample diameter of 5.08 cm. Second, high-temperature (up to 600 °C) dielectric-property measurements were performed on a range of 0.64-cm-thick, 5.08-cm-diameter, commercially supplied ceramic materials, including the α -Al₂O₃ sample from the first experimental campaign.

The experimental error was calculated using a differential uncertainty analysis similar to that described by Baker-Jarvis *et al.* [84], given by the root-sum-square of the uncertainty introduced by the measured magnitude and phase of the scattering parameters, the uncertainty of the sample thickness, and the uncertainty from the aforementioned least squares fitting. This uncertainty calculation procedure is also quite similar to that described by Lighthart [87] for use in dielectric-filled waveguide transmission measurement methods. The error in the scattering parameters was based on the system S-parameter uncertainty given by Agilent for the N5222a network analyzer as a function of frequency and measured power. Error calculations are as follows in (11) and (12), shown at the bottom of the next page, where $\alpha = 11$ or 21, $\Delta|S|$ is the uncertainty in the magnitude of the scattering parameter, $\Delta\theta$ is the uncertainty in the

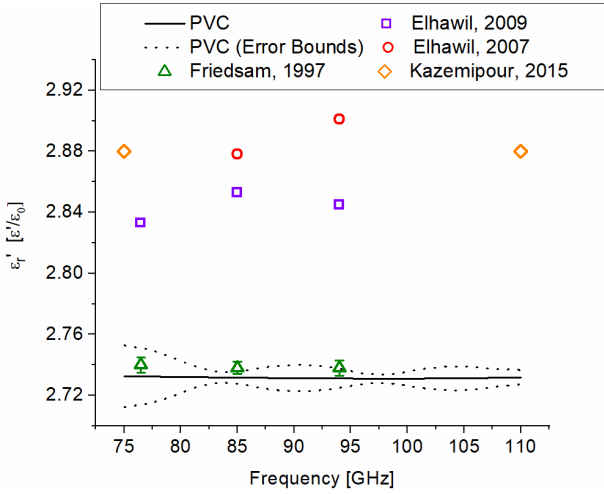


Fig. 5. Measured and literature values of the real portion of the dielectric constant (ϵ'_r) of PVC at W-band (75–110 GHz). Measurements were performed at approximately 25 °C.

phase of the scattering parameter, Δd is the uncertainty in the sample thickness, and the remaining term ($\Delta\epsilon'_{\text{fit}}$ or $\Delta\epsilon''_{\text{fit}}$) is the uncertainty associated with least-squares fitting of the S-parameter data to the transmission line equations. The minimum uncertainty for low-loss materials occurs at multiples of one-half wavelength due to (3) and (5) where $|S_{11}|$ approaches 0 and $|S_{21}|$ approaches 1, which reduces to $z^2 - 1 = 0$. For lossy materials, the error tends to increase at higher frequencies due to decreasing transmitted power and value of $|S_{21}|$.

A. Complex Dielectric Property Measurements of Polyvinyl Chloride at 25 °C

Complex dielectric properties of PVC were measured at 25 °C and compared to previously existing dielectric constant measurement data in the literature [55], [62], [73], [74]. Plots of the real (ϵ'_r) and imaginary (ϵ''_r) permittivity values for the PVC sample, as a function of frequency, are presented in Figs. 5 and 6, respectively. Measured values of the real portion of the dielectric constant agree, within experimental error, with those by Friedsam and Biebl [55] and are within 5% of published values from Elhawil *et al.* [73], [74] and Kazemipour *et al.* [62]. Measured values of the imaginary portion of the dielectric constant agree, within experimental error, with those of [55], [62], and [73]. It is known that the loss tangent of PVC is strongly dependent on small amounts of commonly used low-molecular-weight plasticizers such as tre cresyl phosphate [78].

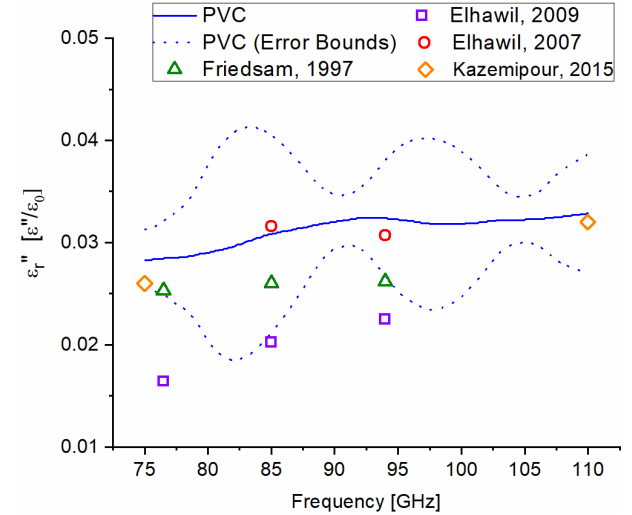


Fig. 6. Measured and literature values of the imaginary portion of the dielectric constant (ϵ''_r) of PVC at W-band (75–110 GHz). Measurements were performed at approximately 25 °C.

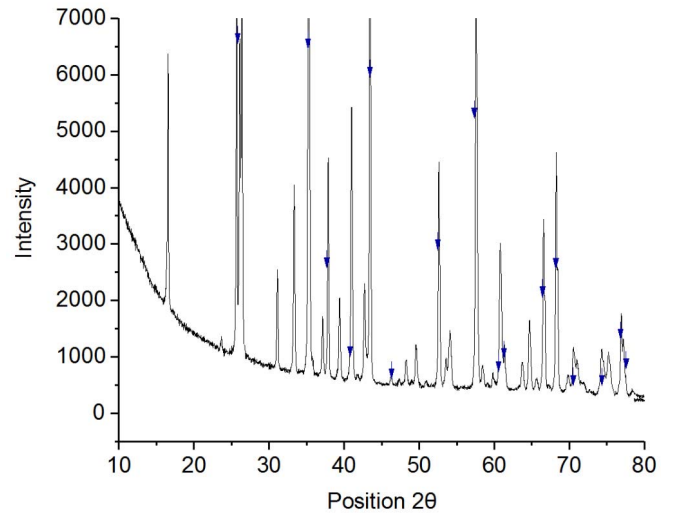


Fig. 7. XRD diffraction pattern of the α -Al₂O₃ substrate. Blue arrows: diffraction peaks of α -Al₂O₃. Unmarked peaks: due to secondary phases, including mullite and silica.

B. Complex Dielectric Property Measurements of 92% α -Al₂O₃ at 25 °C

Prior to performing complex permittivity measurements on the commercial CoorsTek 92% α -Al₂O₃ substrate sample, a compositional analysis was performed. The sample was measured and found to have a density of 3.85 g/cm³. The nonporous substrate is 90.2% of the theoretical density of

$$\frac{\Delta\epsilon'_r}{\epsilon'_r} = \frac{1}{\epsilon'_r} \sqrt{\left(\frac{\partial\epsilon'_r}{\partial|S_\alpha|} \Delta|S_\alpha| \right)^2 + \left(\frac{\partial\epsilon'_r}{\partial|\theta_\alpha|} \Delta\theta_\alpha \right)^2 + \left(\frac{\partial\epsilon'_r}{\partial|d_\alpha|} \Delta d \right)^2 + (\Delta\epsilon'_{\text{fit}})^2} \quad (11)$$

$$\frac{\Delta\epsilon''_r}{\epsilon''_r} = \frac{1}{\epsilon''_r} \sqrt{\left(\frac{\partial\epsilon''_r}{\partial|S_\alpha|} \Delta|S_\alpha| \right)^2 + \left(\frac{\partial\epsilon''_r}{\partial|\theta_\alpha|} \Delta\theta_\alpha \right)^2 + \left(\frac{\partial\epsilon''_r}{\partial|d|} \Delta d \right)^2 + (\Delta\epsilon''_{\text{fit}})^2} \quad (12)$$

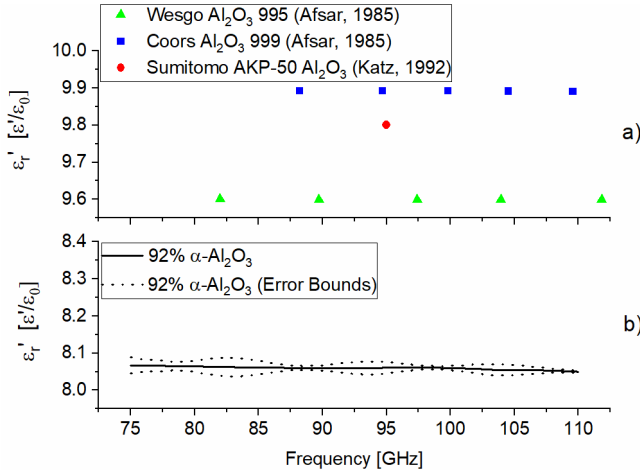


Fig. 8. (a) Literature values of the real portion of the dielectric constant (ϵ_r') of Wesgo Al₂O₃ 995 [51], Coors Al₂O₃ 999 [51], and Sumitomo AKP-50 Al₂O₃ [83] at W-band (75–110 GHz). (b) Measured values of the real portion of the dielectric constant (ϵ_r') of the 92% α -Al₂O₃ at W-band. Measured and literature values are for samples at a temperature of approximately 25 °C.

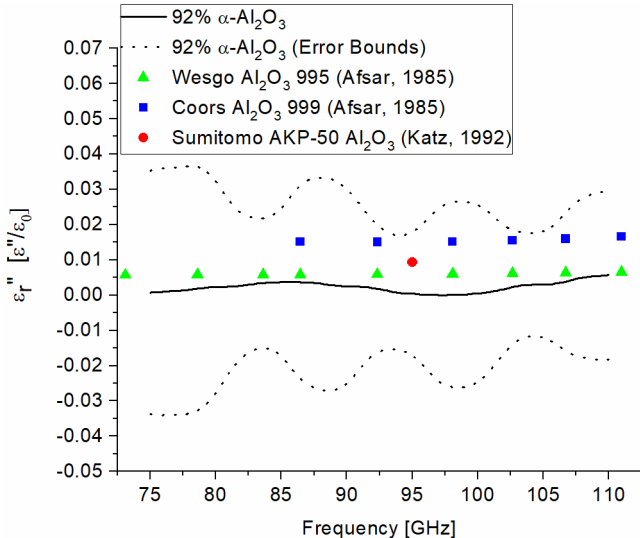


Fig. 9. Measured values of the imaginary portion of the dielectric constant (ϵ_r'') of the 92% α -Al₂O₃ at W-band (75–110 GHz). Literature values of the imaginary portion of the dielectric constant (ϵ_r'') of Wesgo Al₂O₃ 995 [51], Coors Al₂O₃ 999 [51], and Sumitomo AKP-50 Al₂O₃ [83] at W-band are provided for comparison. Measured and literature values are for samples at a temperature of approximately 25 °C. As ϵ_r'' cannot be negative in this material, in regions where the lower error bound extends below zero, the upper error bound represents the threshold below which the present free-space apparatus cannot accurately determine ϵ_r'' .

α -Al₂O₃ (3.96 g/cm³). X-ray diffraction (XRD) was performed on the substrate for phase identification. XRD measurements were performed on a Bruker D-8 Advance (Bruker) using Cu K α radiation. The Bragg–Brentano configuration was used with a scan rate of 3.5° per min over the 2 θ range of 10°–80°. Fig. 7 shows the diffraction pattern with arrows marking the major phase of α -Al₂O₃. A crystalline secondary phase was identified as Al_{4.56}Si_{1.44}O_{9.72}.

Plots of the real (ϵ_r') and imaginary (ϵ_r'') portions of the dielectric constant, as a function of frequency, are presented

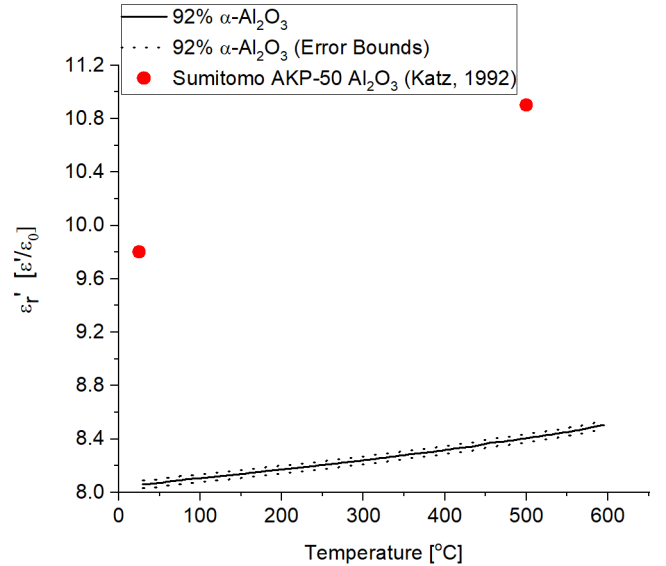


Fig. 10. Measured values of the real portion of the dielectric constant (ϵ_r') of the 92% α -Al₂O₃ at 95 GHz at temperatures ranging from 25 °C to 600 °C. Literature values for Sumitomo AKP-50 Al₂O₃ at 95 GHz [83] are provided for comparison. Temperature uncertainty is ± 7.5 °C.

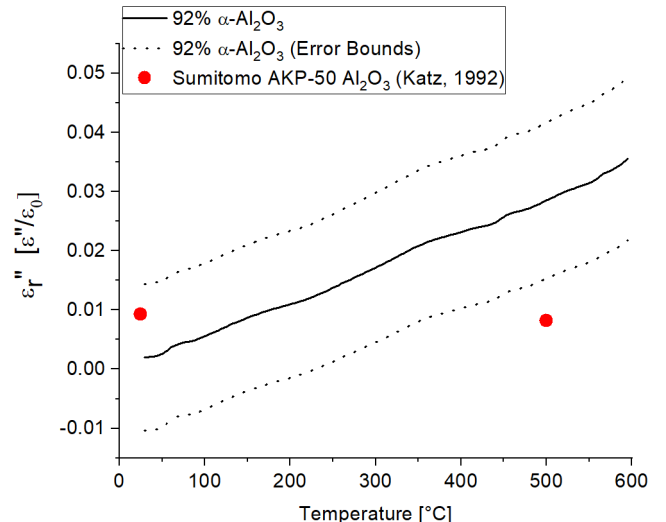


Fig. 11. Measured values of the imaginary portion of the dielectric constant (ϵ_r'') of the 92% α -Al₂O₃ at 95 GHz at temperatures ranging from 25 °C to 600 °C. Literature values for Sumitomo AKP-50 Al₂O₃ at 95 GHz [83] are provided for comparison. As noted previously in the caption of Fig. 9, because ϵ_r'' cannot be negative in this material, in regions where the lower error bound extends below zero, the upper error bound will represent the threshold below which present free-space apparatus cannot accurately determine ϵ_r'' . Temperature uncertainty is ± 7.5 °C.

in Figs. 8(b) and 9, respectively. A slight monotonic decrease in the real part of the dielectric constant, due to dispersion, is evident [88]. Due to the low loss of the α -Al₂O₃ at 25 °C, measurement uncertainties are large compared with the measured values of ϵ_r'' . The authors note that as ϵ_r'' cannot be negative in this material, the upper error bound in Fig. 9 represents the threshold below which the present free-space apparatus cannot accurately determine ϵ_r'' . Literature values of ϵ_r' and ϵ_r'' [Figs. 8(a) and 9, respectively] for Wesgo Al₂O₃ 995 [51],

TABLE I
MEASURED REAL PERMITTIVITY VALUES (ϵ'_r) FOR SELECTED COMMERCIAL CERAMIC SUBSTRATES

Freq.	ϵ'_r (25 °C)	ϵ'_r (150 °C)	ϵ'_r (300 °C)	ϵ'_r (450 °C)	ϵ'_r (600 °C)
Alumina (92% α -Al ₂ O ₃ , CoorsTek, 3.85 g/cm ³)					
75 GHz	8.062 +/- 0.030	8.161 +/- 0.031	8.261 +/- 0.031	8.374 +/- 0.031	8.510 +/- 0.032
95 GHz	8.061 +/- 0.027	8.157 +/- 0.027	8.255 +/- 0.027	8.366 +/- 0.028	8.501 +/- 0.028
110 GHz	8.059 +/- 0.024	8.155 +/- 0.024	8.252 +/- 0.025	8.363 +/- 0.025	8.499 +/- 0.026
Zirconium Oxide (99.9%, American Elements, 5.60 g/cm ³)					
75 GHz	23.52 +/- 0.10	23.68 +/- 0.10	24.13 +/- 0.11	24.77 +/- 0.12	25.39 +/- 0.15
95 GHz	23.52 +/- 0.10	23.67 +/- 0.10	24.12 +/- 0.11	24.76 +/- 0.12	25.36 +/- 0.14
110 GHz	23.52 +/- 0.10	23.67 +/- 0.10	24.12 +/- 0.10	24.75 +/- 0.11	25.35 +/- 0.14
Boron Nitride (99.5%, Stanford Advanced Materials, 1.96 g/cm ³)					
75 GHz	4.184 +/- 0.025	4.179 +/- 0.025	4.174 +/- 0.025	4.179 +/- 0.025	4.208 +/- 0.025
95 GHz	4.183 +/- 0.022	4.178 +/- 0.021	4.173 +/- 0.021	4.177 +/- 0.021	4.205 +/- 0.022
110 GHz	4.178 +/- 0.026	4.173 +/- 0.026	4.167 +/- 0.025	4.171 +/- 0.025	4.199 +/- 0.026
Silicon Nitride (99.5%, American Elements, 2.17 g/cm ³)					
75 GHz	5.150 +/- 0.033	5.159 +/- 0.033	5.188 +/- 0.033	5.220 +/- 0.034	5.251 +/- 0.034
95 GHz	5.143 +/- 0.029	5.152 +/- 0.029	5.181 +/- 0.029	5.211 +/- 0.029	5.241 +/- 0.029
110 GHz	5.138 +/- 0.026	5.146 +/- 0.026	5.175 +/- 0.026	5.204 +/- 0.026	5.234 +/- 0.027

TABLE II
MEASURED IMAGINARY PERMITTIVITY VALUES (ϵ''_r) FOR SELECTED COMMERCIAL CERAMIC SUBSTRATES

Freq.	ϵ''_r (25 °C)	ϵ''_r (150 °C)	ϵ''_r (300 °C)	ϵ''_r (450 °C)	ϵ''_r (600 °C)
Alumina (92% α -Al ₂ O ₃ , CoorsTek, 3.85 g/cm ³)					
75 GHz	< 0.010	0.011 +/- 0.008	0.020 +/- 0.009	0.027 +/- 0.009	0.037 +/- 0.009
95 GHz	< 0.009	0.012 +/- 0.008	0.020 +/- 0.008	0.027 +/- 0.008	0.035 +/- 0.008
110 GHz	< 0.008	0.013 +/- 0.007	0.020 +/- 0.008	0.025 +/- 0.008	0.032 +/- 0.008
Zirconium Oxide (99.9%, American Elements, 5.60 g/cm ³)					
75 GHz	0.228 +/- 0.056	0.259 +/- 0.057	0.369 +/- 0.062	0.621 +/- 0.071	1.010 +/- 0.086
95 GHz	0.236 +/- 0.052	0.268 +/- 0.053	0.378 +/- 0.057	0.626 +/- 0.066	1.007 +/- 0.081
110 GHz	0.247 +/- 0.047	0.273 +/- 0.048	0.384 +/- 0.054	0.629 +/- 0.064	1.004 +/- 0.079
Boron Nitride (99.5%, Stanford Advanced Materials, 1.96 g/cm ³)					
75 GHz	< 0.024	< 0.025	< 0.025	< 0.026	0.014 +/- 0.014
95 GHz	0.016 +/- 0.015	0.017 +/- 0.015	0.018 +/- 0.015	0.020 +/- 0.015	0.021 +/- 0.015
110 GHz	0.018 +/- 0.010	0.020 +/- 0.010	0.021 +/- 0.010	0.022 +/- 0.010	0.022 +/- 0.010
Silicon Nitride (99.5%, American Elements, 2.17 g/cm ³)					
75 GHz	0.080 +/- 0.009	0.082 +/- 0.009	0.088 +/- 0.009	0.095 +/- 0.009	0.101 +/- 0.009
95 GHz	0.081 +/- 0.008	0.083 +/- 0.008	0.089 +/- 0.008	0.095 +/- 0.008	0.101 +/- 0.007
110 GHz	0.081 +/- 0.007	0.084 +/- 0.007	0.089 +/- 0.007	0.095 +/- 0.007	0.101 +/- 0.007

Coors Al₂O₃ 999 [51], and Sumitomo AKP-50 Al₂O₃ [83] at W-band are provided for comparison. Purity values for the Wesgo 995, Coors 999, and Sumitomo AKP-50 are 99.5%, 99.9%, and 99.995%, respectively, [83], [89].

The W-band measured real permittivity values (ϵ'_r) of the 92% α -Al₂O₃ sample were found to be lower than the published literature values of Al₂O₃ plotted in Fig. 8(a). The presence of lower-permittivity silica

($\epsilon'_r \approx 3.8$ @ 1 GHz) [11] and mullite ($\epsilon'_r \approx 6.5$ @ 1 GHz) [12] secondary phases detected in the 92% α -Al₂O₃ sample would be expected to reduce the bulk-averaged value of the real permittivity, compared with higher-purity alumina. At 25 °C, measured, W-band, imaginary permittivity values of the 92% α -Al₂O₃ sample were found to be below the measurement threshold for the present experimental configuration.

C. Measurement of Samples at Temperatures Up to 600 °C

As part of the high-temperature dielectric measurement series, four commercially available ceramic substrates, including the CoorsTek 92% α -Al₂O₃ sample, were characterized at temperatures ranging from 25 °C to 600 °C. The additional three ceramic substrates were composed of 99.9% zirconium oxide (American Elements, 5.60 g/cm³), 99.5% boron nitride (Stanford Advanced Materials, 1.96 g/cm³), and 99.5% silicon nitride (American Elements, 2.17 g/cm³), respectively. Figs. 10 and 11 provide high-temperature complex permittivity data (ϵ'_r in Fig. 10 and ϵ''_r in Fig. 11) for the 92% α -Al₂O₃ sample at 95 GHz. Literature values for Sumitomo AKP-50 Al₂O₃ at 25 °C and 500 °C [83] are provided for comparison.

In the 25 °C–600 °C temperature range, both the real and imaginary portions of the permittivity of the 92% α -Al₂O₃ increased monotonically as a function of temperature as the conductivity of the material increased. Real permittivity (ϵ'_r) increased 5.5% from 8.061 ± 0.027 to 8.501 ± 0.028 , and imaginary permittivity increased from <0.009 to 0.035 ± 0.008 . The temperature dependence of the real part of the permittivity of aluminum oxide, shown by Harrop to have a coefficient of capacitance of approximately 110 ppm/°C, is attributed to ionic polarization [90]. For aluminum oxide, an increase in temperature from 25 °C to 600 °C is predicted to yield an increase in ϵ'_r of approximately 6.3% [90], which is close to the observed increase in ϵ'_r of the 92% α -Al₂O₃ (5.2%).

Measured real (ϵ'_r) and imaginary (ϵ''_r) permittivity data for the four commercial ceramic substrates are provided in Tables I and II, respectively. Measured values are provided for 75, 95, and 110 GHz at temperatures ranging from 25 °C to 600 °C. Manufacturer information on purity and measured density data are also provided for each sample material.

V. CONCLUSION

Development of the next-generation, high-power, *W*-band systems requires an understanding of the dielectric properties of insulating materials, including ceramics and polymers, at elevated temperatures. Free-space measurement techniques can be contactless and can accommodate large, flat sheets of dielectric sample material, making them useful for characterization of high-temperature millimeter-wave window and radome candidate materials. As part of the present work, a high-temperature, free-space measurement system was developed and used to characterize complex dielectric properties of bulk material samples at temperatures ranging from 25 °C to 600 °C.

Two test cases, PVC and 92% α -Al₂O₃, were measured at 25 °C and found to have ϵ'_r values of 2.731 ± 0.005 and 8.061 ± 0.027 at 95 GHz, respectively. The 25 °C PVC sample was measured to have ϵ''_r value of 0.032 ± 0.007 . At 25 °C, ϵ''_r of the α -Al₂O₃ sample was below the uncertainty threshold achievable with the present free-space measurement apparatus and could only be bounded to <0.009 . When the α -Al₂O₃ sample was heated to 600 °C, ϵ'_r and ϵ''_r values increased to 8.501 ± 0.028 and 0.035 ± 0.008 , respectively. The observed increase of the real part of the permittivity of the 92% α -Al₂O₃

ceramic (5.5%) over the 25 °C–600 °C range was found to be consistent with predictions based on [90] (6.3%).

Using the same measurement procedure developed for the α -Al₂O₃ sample, three additional commercially available ceramic substrates (zirconium oxide, boron nitride, and silicon nitride) were characterized at temperatures ranging from 25 °C to 600 °C. At 95 GHz, the zirconium oxide sample showed an increase in permittivity of 7.8% over the 25 °C–600 °C temperature range, while the boron nitride and silicon nitride samples showed more modest increases in real permittivity of 0.7% and 1.9%, respectively. At 95 GHz, the imaginary permittivity of the zirconium oxide increased by 0.771. The measured imaginary permittivity of the silicon nitride increased by 0.020 ± 0.008 over the 25 °C–600 °C temperature range. The boron nitride sample showed negligible change in imaginary permittivity, to within calculated uncertainty, at 95 GHz, when heated from 25 °C to 600 °C.

ACKNOWLEDGMENT

The authors would like to thank A. Sayir of the Air Force Office of Scientific Research for his helpful discussion. B. Jawdat contributed to this effort while holding an NRC Research Associateship Award at The Air Force Research Laboratory. Z. W. Cohick and J. M. Gaone contributed to this effort while participating in the Air Force Research Laboratory Directed Energy Scholars Program.

REFERENCES

- [1] W. W. Camp, J. T. Mayhan, and R. M. O'Donnell, "Wideband radar for ballistic missile defense and range-Doppler imaging of satellites," *Lincoln Lab. J.*, vol. 12, no. 2, pp. 267–280, 2000.
- [2] N. Kumar, U. Singh, A. Kumar, and A. K. Sinha, "Design of 95 GHz, 100 kW gyrotron for active denial system application," *Vacuum*, vol. 99, pp. 99–106, Jan. 2013.
- [3] S. Levine, "The active denial system: A revolutionary, non-lethal weapon for today's battlefield," Nat. Defense Univ., Washington, DC, USA, Tech. Rep. ADA501865, Jun. 2009.
- [4] M. S. Venkatesh and G. S. V. Raghavan, "An overview of dielectric properties measuring techniques," *Can. Biosyst. Eng.*, vol. 47, no. 7, pp. 15–30, Jan. 2005.
- [5] J. W. Lamb, "Miscellaneous data on materials for millimetre and submillimetre optics," *Int. J. Infr. Millim. Waves*, vol. 17, no. 12, pp. 1997–2034, Dec. 1996.
- [6] G. J. Simonis, "Index to the literature dealing with the near-millimeter wave properties of materials," *Int. J. Infr. Millim. Waves*, vol. 3, no. 4, pp. 439–469, Jul. 1982.
- [7] J. W. Schultz, *Focused Beam Methods: Measuring Microwave Materials in Free Space*. Atlanta, GA, USA, 2012.
- [8] J. Sheen, "Comparisons of microwave dielectric property measurements by transmission/reflection techniques and resonance techniques," *Meas. Sci. Technol.*, vol. 20, no. 4, Jan. 2009, Art. no. 042001.
- [9] J. P. Calame, M. Garven, D. Lobas, R. E. Myers, F. Wood, and D. K. Abe, "Broadband microwave and W-band characterization of Be-O-SiC and AlN-based lossy dielectric composites for vacuum electronics," in *Proc. IEEE Int. Vacuum Electron Sources*, Apr. 2006, pp. 37–38.
- [10] R. J. Cook and R. G. Jones, "Precise dielectric measurement techniques for the frequency range 10 GHz to 150 GHz," in *Proc. 8th Eur. Microw. Conf.*, Sep. 1978, pp. 528–532.
- [11] W. B. Westphal and A. Sils, "Dielectric constant and loss data," Massachusetts Inst. Technol., Cambridge, MA, USA, Tech. Rep. AD746686, 1972.
- [12] W. B. Westphal, "High-temperature dielectric measurements on radome ceramics in the microwave region," Massachusetts Inst. Technol., Cambridge, MA, USA, Tech. Rep. AD122938, 1957.

- [13] M. N. Afsar, J. R. Birch, R. N. Clarke, and G. W. Chantry, "The measurement of the properties of materials," *Proc. IEEE*, vol. 74, no. 1, pp. 183–199, Jan. 1986.
- [14] J. R. Birch and R. N. Clarke, "Dielectric and optical measurements from 30 to 1000 GHz," *Radio Electron. Eng.*, vol. 52, nos. 11–12, pp. 565–584, 1982.
- [15] R. N. Clarke and C. B. Rosenberg, "Fabry-Perot and open resonators at microwave and millimetre wave frequencies, 2–300 GHz," *J. Phys. E, Sci. Instrum.*, vol. 15, no. 1, pp. 9–24, 1982.
- [16] T. Zwick, A. Chandrasekhar, C. W. Baks, U. R. Pfeiffer, S. Brebels, and B. P. Gaucher, "Determination of the complex permittivity of packaging materials at millimeter-wave frequencies," *IEEE Trans. Microw. Theory Techn.*, vol. 54, no. 3, pp. 1001–1009, Mar. 2006.
- [17] J. R. Izatt and F. Kremer, "Millimeter wave measurement of both parts of the complex index of refraction using an untuned cavity resonator," *Appl. Opt.*, vol. 20, no. 14, pp. 2555–2559, 1981.
- [18] M. Garven, J. P. Calame, B. Myers, and D. Lobas, "Variable temperature measurements of the dielectric properties of lossy materials in W-band," in *Proc. Joint 30th Int. Conf. Infr. Millim. Waves 13th Int. Conf. Terahertz Electron.*, vol. 1, Sep. 2005, pp. 174–175.
- [19] W. W. Ho, "High temperature millimeter wave characterization of the dielectric properties of advanced window materials," DTIC, Fort Belvoir, VA, USA, Tech. Rep. AMMRC TR 8, 1982.
- [20] W. W. Ho, "Millimeter wave dielectric property measurement of gyrotron window materials," Thousand Oaks, CA, USA, ORNL Tech. Rep., 1985.
- [21] W. W. Ho, "Millimeter wave dielectric property measurement of gyrotron window materials," Thousand Oaks, CA, USA, ORNL Tech. Rep., 1984.
- [22] M. T. Lanagan, J. K. Yamamoto, A. Bhalla, and S. G. Sankar, "The dielectric properties of yttria-stabilized zirconia," *Mater. Lett.*, vol. 7, no. 12, pp. 437–440, 1989.
- [23] M. Mirsaneh, E. Furman, J. V. Ryan, M. T. Lanagan, and C. G. Pantano, "Frequency dependent electrical measurements of amorphous GeSbSe chalcogenide thin films," *Appl. Phys. Lett.*, vol. 96, no. 11, 2010, Art. no. 112907.
- [24] S. Roberts and A. von Hippel, "A new method for measuring dielectric constant and loss in the range of centimeter waves," *J. Appl. Phys.*, vol. 17, no. 7, pp. 610–616, Apr. 1946.
- [25] U. Stumper, "A TE_{01n} cavity resonator method to determine the complex permittivity of low loss liquids at millimeter wavelengths," *Rev. Sci. Instrum.*, vol. 44, no. 2, pp. 165–169, 1973.
- [26] J. R. Birch *et al.*, "An intercomparison of measurement techniques for the determination of the dielectric properties of solids at near millimetre wavelengths," *IEEE Trans. Microw. Theory Techn.*, vol. 42, no. 6, pp. 956–965, Jun. 1994.
- [27] W. B. Bridges, M. B. Klein, and E. Schweig, "Measurement of the dielectric constant and loss tangent of thallium mixed halide crystals KRS-5 and KRS-6 at 95 GHz," *IEEE Trans. Microw. Theory Techn.*, vol. 30, no. 3, pp. 286–292, Mar. 1982.
- [28] R. I. Hunter, D. A. Robertson, and G. M. Smith, "Waveguide characterization of various solid absorbing materials at W-band," *IEEE Microw. Wireless Compon. Lett.*, vol. 21, no. 7, pp. 389–391, Jul. 2011.
- [29] M. T. Lanagan, J. H. Kim, D. C. Dube, S. J. Jang, and R. E. Newnham, "A microwave dielectric measurement technique for high permittivity materials," *Ferroelectrics*, vol. 82, no. 1, pp. 91–97, 1988.
- [30] H. Soleimani, Z. Abbas, N. Yahya, H. Soleimani, and M. Y. Ghotbi, "Determination of complex permittivity and permeability of lanthanum iron garnet filled PVDF-polymer composite using rectangular waveguide and Nicholson-Ross-Weir (NRW) method at X-band frequencies," *Measurement*, vol. 45, no. 6, pp. 1621–1625, 2012.
- [31] M. N. Afsar, "Precision millimeter-wave dielectric measurements of birefringent crystalline sapphire and ceramic alumina," *IEEE Trans. Instrum. Meas.*, vol. IM-36, no. 2, pp. 554–559, Jun. 1987.
- [32] M. N. Afsar, "Precision millimeter-wave measurements of complex refractive index, complex dielectric permittivity, and loss tangent of common polymers," *IEEE Trans. Instrum. Meas.*, vol. IM-36, no. 2, pp. 530–536, Jun. 1987.
- [33] M. N. Afsar and H. Chi, "Window materials for high power gyrotron," *Int. J. Infr. Millim. Waves*, vol. 15, no. 7, pp. 1161–1179, 1994.
- [34] M. N. Afsar and H. Chi, "Millimeter wave complex refractive index, complex dielectric permittivity and loss tangent of extra high purity and compensated silicon," *Int. J. Infr. Millim. Waves*, vol. 15, no. 7, pp. 1181–1188, 1994.
- [35] M. N. Afsar, I. I. Tkachov, and K. N. Kocharyan, "A novel W-band spectrometer for dielectric measurements," *IEEE Trans. Microw. Theory Techn.*, vol. 48, no. 12, pp. 2637–2643, Dec. 2000.
- [36] M. N. Afsar, Y. Wang, and A. Moonshiram, "Measurement of transmittance and permittivity of dielectric materials using dispersive Fourier transform spectroscopy," *Microw. Opt. Technol. Lett.*, vol. 38, no. 1, pp. 27–30, Jul. 2003.
- [37] M. N. Afsar, K. A. Korolev, L. Subramanian, and I. I. Tkachov, "Complex dielectric measurements of materials at Q-band, V-band and W-band frequencies with high power sources," in *Proc. IEEE Instrum. Meas. Technol. Conf.*, vol. 1, May 2005, pp. 82–87.
- [38] M. N. Afsar, K. Wang, P. Liu, and K. A. Korolev, "Permittivity of highly absorbing oxide ceramics in millimeter waves," in *Proc. 33rd Int. Conf. Infrared, Millim. Terahertz Waves*, Sep. 2008, pp. 1–2.
- [39] M. J. Bangham *et al.*, "Physical measurement in the 100–1000 GHz frequency range," *Radio Electron. Eng.*, vol. 49, no. 7, pp. 403–418, Dec. 1979.
- [40] N. I. Furashov, V. E. Dudin, and B. A. Sverdlov, "Spectral measurements of dielectric characteristics of petroleum and petroleum oils in the millimeter wave range," *Radiophys. Quantum Electron.*, vol. 50, no. 6, pp. 442–451, Jul. 2007.
- [41] K. A. Korolev, S. Chen, and M. N. Afsar, "Complex magnetic permeability and dielectric permittivity of ferrites in millimeter waves," *IEEE Trans. Magn.*, vol. 44, no. 4, pp. 435–437, Apr. 2008.
- [42] K. A. Korolev, S. Chen, and M. N. Afsar, "Precision transmittance measurements on ferrites in millimeter waves," in *Proc. Conf. Precis. Electromagn. Meas. Dig.*, Jun. 2008, pp. 536–537.
- [43] K. A. Korolev and M. N. Afsar, "Magnetic properties of nanoferrites near ferromagnetic resonance in millimeter waves," *IEEE Trans. Magn.*, vol. 47, no. 10, pp. 4120–4123, Oct. 2011.
- [44] K. N. Kocharyan, M. N. Afsar, and I. I. Tkachov, "New method for measurement of complex magnetic permeability in the millimeter-wave range, part II: Hexaferrites," *IEEE Trans. Magn.*, vol. 35, no. 4, pp. 2104–2110, Jul. 1999.
- [45] K. N. Kocharyan, M. Afsar, and I. I. Tkachov, "Millimeter-wave magnetooptics: New method for characterization of ferrites in the millimeter-wave range," *IEEE Trans. Microw. Theory Techn.*, vol. 47, no. 12, pp. 2636–2643, Dec. 1999.
- [46] Z. Li, A. I. M. Ayala, M. N. Afsar, and K. A. Korolev, "Free space quasi-optical instrumentation for dielectric measurements of highly scattering materials in millimeter waves," in *Proc. IEEE Instrum. Meas. Technol. Conf.*, May 2009, pp. 607–611.
- [47] M. N. Afsar, J. Chamberlain, and G. W. Chantry, "High-precision dielectric measurements on liquids and solids at millimeter and submillimeter wavelengths," *IEEE Trans. Instrum. Meas.*, vol. IM-25, no. 4, pp. 290–294, 1976.
- [48] M. N. Afsar and K. J. Button, "Millimeter and submillimeter wave measurements of complex optical and dielectric parameters of materials," *Int. J. Infr. Millim. Waves*, vol. 3, no. 6, pp. 929–939, Nov. 1982.
- [49] M. N. Afsar and K. J. Button, "Precise millimeter-wave measurements of complex refractive index, complex dielectric permittivity and loss tangent of GaAs, Si, SiO₂, Al₂O₃, BeO, Macor, and glass," *IEEE Trans. Microw. Theory Techn.*, vol. MTT-31, no. 2, pp. 217–223, Feb. 1983.
- [50] M. N. Afsar, "Dielectric measurements of millimeter-wave materials," *IEEE Trans. Microw. Theory Techn.*, vol. MTT-32, no. 12, pp. 1598–1609, Dec. 1984.
- [51] M. N. Afsar and K. J. Button, "Millimeter-wave dielectric measurement of materials," *Proc. IEEE*, vol. 73, no. 1, pp. 131–153, Jan. 1985.
- [52] M. N. Afsar, "Precision dielectric measurements of nonpolar polymers in the millimeter wavelength range," *IEEE Trans. Microw. Theory Techn.*, vol. MTT-33, no. 12, pp. 1410–1415, Dec. 1985.
- [53] R. Böhmer, M. Maglione, P. Lunkenheimer, and A. Loidl, "Radio-frequency dielectric measurements at temperatures from 10 to 450 K," *J. Appl. Phys.*, vol. 65, no. 3, pp. 901–904, Feb. 1989.
- [54] O. Tantot, M. Chatard-Moulin, and P. Guillon, "Measurement of complex permittivity and permeability and thickness of multilayered medium by an open-ended waveguide method," *IEEE Trans. Instrum. Meas.*, vol. 46, no. 2, pp. 519–522, Apr. 1997.
- [55] G. L. Friedsam and E. M. Biebl, "Precision free-space measurements of complex permittivity of polymers in the W-band," in *IEEE MTT-S Int. Microw. Symp. Dig.*, vol. 3, Jun. 1997, pp. 1351–1354.
- [56] D. K. Ghodgaonkar, V. V. Varadan, and V. K. Varadan, "A free-space method for measurement of dielectric constants and loss tangents at microwave frequencies," *IEEE Trans. Instrum. Meas.*, vol. 38, no. 3, pp. 789–793, Jun. 1989.

- [57] D. K. Ghodgaonkar, V. V. Varadan, and V. K. Varadan, "Free-space measurement of complex permittivity and complex permeability of magnetic materials at microwave frequencies," *IEEE Trans. Instrum. Meas.*, vol. 39, no. 2, pp. 387–394,
- [58] K. Godziszewski and Y. Yashchyshyn, "Investigation of influence of measurement conditions on accuracy of material characterization in sub-THz frequency range," in *Proc. 21st Int. Conf. Microw., Radar Wireless Commun.*, May 2016, pp. 1–4.
- [59] R. D. Hollinger, K. A. Jose, A. Tellakula, V. V. Varadan, and V. K. Varadan, "Microwave characterization of dielectric materials from 8 to 110 GHz using a free-space setup," *Microw. Opt. Technol. Lett.*, vol. 26, no. 2, pp. 100–105, Jul. 2000.
- [60] T.-W. Kang, J.-H. Kim, D.-J. Lee, and N.-W. Kang, "Free-space measurement of the complex permittivity of liquid materials at millimeter-wave region," in *Proc. Conf. Precis. Electromagn. Meas.*, Jul. 2016, pp. 1–2.
- [61] A. Kazemipour, M. Hudlička, M. Salhi, T. Kleine-Ostmann, and T. Schrader, "Free-space quasi-optical spectrometer for material characterization in the 50–500 GHz frequency range," in *Proc. 44th Eur. Microw. Conf.*, Oct. 2014, pp. 636–639.
- [62] A. Kazemipour *et al.*, "Design and calibration of a compact quasi-optical system for material characterization in millimeter/submillimeter wave domain," *IEEE Trans. Instrum. Meas.*, vol. 64, no. 6, pp. 1438–1445, Jun. 2015.
- [63] A. Kazemipour, M. Hudlička, T. Kleine-Ostmann, and T. Schrader, "A reliable simple method to extract the intrinsic material properties in millimeter/sub-millimeter wave domain," in *Proc. 29th Conf. Precis. Electromagn. Meas.*, Aug. 2014, pp. 576–577.
- [64] D. Lemaire, D. Cros, H. Jallageas, and P. Guillou, "Material characterisation from -160°C up to 800°C in centimeter and millimeter wavelength frequency band," in *Proc. 20th Biennial Conf. Precis. Electromagn. Meas.*, Jun. 1996, pp. 72–73.
- [65] D. Bourreau, A. Péden, and S. Le Maguer, "A quasi-optical free-space measurement setup without time-domain gating for material characterization in the W-band," *IEEE Trans. Instrum. Meas.*, vol. 55, no. 6, pp. 2022–2028, Dec. 2006.
- [66] F. I. Shimabukuro, S. Lazar, M. R. Chernick, and H. B. Dyson, "A quasi-optical method for measuring the complex permittivity of materials," *IEEE Trans. Microw. Theory Techn.*, vol. MTT-32, no. 7, pp. 659–665, Jul. 1984.
- [67] F. I. Shimabukuro, "Correction to 'Quasi-optical method for measuring the complex permittivity of materials,'" *IEEE Trans. Microw. Theory Techn.*, vol. MTT-32, no. 11, p. 1504, Nov. 1984.
- [68] F. I. Shimabukuro and S. Lazar, "Measurement of the complex dielectric constant of casting resins at millimeter wavelengths low-loss," in *IEEE MTT-S Int. Microw. Symp. Dig.*, May/Jun. 1984, pp. 520–521.
- [69] V. V. Varadan, R. D. Hollinger, D. K. Ghodgaonkar, and V. K. Varadan, "Free-space, broadband measurements of high-temperature, complex dielectric properties at microwave frequencies," *IEEE Trans. Instrum. Meas.*, vol. 40, no. 5, pp. 842–846, Oct. 1991.
- [70] W. W. Ho, "High-temperature dielectric properties of polycrystalline ceramics," *MRS Online Proc. Library*, vol. 124, pp. 137–148, Jan. 1988.
- [71] S. Chen, K. A. Korolev, J. Kupershmidt, K. Nguyen, and M. N. Afsar, "High-resolution high-power quasi-optical free-space spectrometer for dielectric and magnetic measurements in millimeter waves," *IEEE Trans. Instrum. Meas.*, vol. 58, no. 8, pp. 2671–2678, Aug. 2009.
- [72] R. W. Cravey and P. I. Tiemsin, "W-band transmission measurements and X-band dielectric properties measurements for a radome sample," *Nasa Tech. Memorandum* 110321, Feb. 1997.
- [73] A. Elhawil, G. Koers, L. Zhang, J. Stiens, and R. Vounckx, "Reliable method for material characterisation using quasi-optical free-space measurement in W-band," *Sci. Meas. Technol.*, vol. 3, no. 1, pp. 39–50, Feb. 2009.
- [74] A. Elhawil *et al.*, "A quasi-optical free-space method for dielectric constant characterization of polymer materials in mm-wave band," in *Proc. Symp. IEEE/LEOS Benelux Chapter*, vol. 66, pp. 187–190, Dec. 2007.
- [75] A. Elhawil, G. Koers, L. Zhang, J. Stiens, and R. Vounckx, "Comparison between two optimisation algorithms to compute the complex permittivity of dielectric multilayer structures using a free-space quasi-optical method in W-band," *Sci. Meas. Technol.*, vol. 3, no. 1, pp. 13–21, Jan. 2009.
- [76] D. T. Fralick, "W-band free space permittivity measurement setup for candidate radome materials," *NASA Contractor Rep.* 201720, Aug. 1997.
- [77] G. L. Friedsam and E. M. Biebl, "A broadband free-space dielectric properties measurement system at millimeter wavelengths," *IEEE Trans. Instrum. Meas.*, vol. 46, no. 2, pp. 515–518, Apr. 1997.
- [78] A. J. Bur, "Dielectric properties of polymers at microwave frequencies: A review," *Polymer*, vol. 26, no. 7, pp. 963–977, Jul. 1985.
- [79] M. Lee, "Dielectric constant and loss tangent in LiNbO_3 crystals from 90 to 147 GHz," *Appl. Phys. Lett.*, vol. 79, no. 9, pp. 1342–1344, Aug. 2001.
- [80] D. Grischkowsky, S. Keiding, M. van Exter, and C. Fattinger, "Far-infrared time-domain spectroscopy with terahertz beams of dielectrics and semiconductors," *J. Opt. Soc. Amer. B, Opt. Phys.*, vol. 7, no. 10, pp. 2006–2015, Oct. 1990.
- [81] U. Kaatze, "Measuring the dielectric properties of materials. Ninety-year development from low-frequency techniques to broadband spectroscopy and high-frequency imaging," *Meas. Sci. Technol.*, vol. 24, no. 1, Dec. 2012, Art. no. 012005.
- [82] R. van Loon and R. Finsy, "Measurement of complex permittivity of liquids at frequencies from 60 to 150 GHz," *Rev. Sci. Instrum.*, vol. 45, no. 4, pp. 523–525, Apr. 1974.
- [83] J. D. Katz, "Microwave sintering of ceramics," *Annu. Rev. Mater. Sci.*, vol. 22, no. 1, pp. 153–170, Aug. 1992.
- [84] J. Baker-Jarvis, E. J. Vanzura, and W. A. Kissick, "Improved technique for determining complex permittivity with the transmission/reflection method," *IEEE Trans. Microw. Theory Techn.*, vol. 38, no. 8, pp. 1096–1103, Aug. 1990.
- [85] "Basics of measuring the dielectric properties of materials," Keysight Technologies, Santa Rosa, CA, USA, 2017.
- [86] M. T. Lanagan, M. T. Kim, S. J. Jang, and R. E. Newnham, "Microwave dielectric properties of antiferroelectric lead zirconate," *J. Amer. Ceram. Soc.*, vol. 71, no. 4, pp. 311–316, Apr. 1988.
- [87] L. P. Ligthart, "A fast computational technique for accurate permittivity determination using transmission line methods," *IEEE Trans. Microw. Theory Techn.*, vol. MTT-31, no. 3, pp. 249–254, Mar. 1983.
- [88] A. R. Von Hippel, *Dielectric Materials and Applications*, 2nd ed. Boston, MA, USA: Artech House, 1995.
- [89] K. J. Button, *Infrared and Millimeter Waves*. Orlando, FL, USA: Academic, 1984.
- [90] P. J. Harrop, "Temperature coefficients of capacitance of solids," *J. Mater. Sci.*, vol. 4, no. 4, pp. 370–374, Apr. 1969.